Available online at www.sciencedirect.com
SCIENCE DIRECT®
Physics Letters B 638 (2006) 382–387
PHYSICS LETTERS B
www.elsevier.com/locate/physletb

Holographic model at finite temperature with R-charge density

Kazuo Ghoroku [a,*], Akihiro Nakamura [b], Masanobu Yahiro [c]

[a] *Fukuoka Institute of Technology, Wajiro, Higashi-ku, Fukuoka 811-0295, Japan*
[b] *Department of Physics, Kagoshima University, Korimoto 1-21-35, Kagoshima 890-0065, Japan*
[c] *Department of Physics, Kyushu University, Hakozaki, Higashi-ku, Fukuoka 812-8581, Japan*

Received 4 May 2006; received in revised form 23 May 2006; accepted 25 May 2006

Available online 9 June 2006

Editor: M. Cvetič

Abstract

We consider a holographic model of QCD at finite temperature with nonzero chemical potentials conjugate to R-charge densities. A critical surface of the confinement–deconfinement phase transition is shown for five-dimensional charged black hole solution given by Behrndt, Cvetič and Sabra. On a special section of the parameter space, we find a critical curve being similar to the one expected in QCD. We calculate meson spectra and decay constants in the confinement phase of this section to see their temperature and chemical potential dependences. We could assure generalized Gell-Mann–Oakes–Renner relation and the reduction of pion velocity near the critical point.

1. Introduction

Recently, from the gravity/gauge correspondence [1], the probe brane approach to the gauge theory with flavor quarks has been largely developed in terms of the system of D_p/D_{p+4} branes [2,3]. Inspired by these works, phenomenological, 5d holographic models have been proposed to explain more quantitative properties of light mesons in a simple setting [4–8]. And a simple model proposed in [4,5] is extended to the finite-temperature version [9], which could cover both the confinement and the deconfinement phase.

On the other hand, the thermal gauge theories with chemical potentials conjugate to R-charges densities have been studied in the framework of the gauge/gravity correspondence [10–17]. While the charge in such theories is not the one of QCD, it would be an interesting problem to apply our previous model [9] to these theories and to see the flavor meson properties in a thermal medium with chemical potentials conjugate to these charge densities.

Among the models with R-charges, we consider here the background configuration which has been found by Behrndt, Cvetič and Sabra [10] as a solution to the equations of motion of the five-dimensional $\mathcal{N} = 2$ gauged supergravity. This solution is corresponding to the dimensional reduction of the spinning three-brane, and it is characterized by three chemical potentials and a horizon. The analyses are given here on a special section of these parameter space to study the dynamical role of these chemical potentials in the various quantities related to quark and meson.

In the next section, we set our holographic model of R-charge induced chemical potential. And a phase diagram, which is very similar to the one expected in QCD, of this model is given. In Section 3, various light meson properties are given and we find many interesting results, especially near the critical curve of confinement and deconfinement. And the summary is given in the final section.

2. Model setting

We use the R-charged black hole solution to equations of motion of the five-dimensional $\mathcal{N} = 2$ gauged supergravity found by Behrndt, Cvetič and Sabra [10]. The background for

* Corresponding author.
E-mail addresses: gouroku@dontaku.fit.ac.jp, gouroku@fit.ac.jp (K. Ghoroku), nakamura@sci.kagoshima-u.ac.jp (A. Nakamura), yahiro2scp@mbox.nc.kyushu-u.ac.jp (M. Yahiro).

0370-2693
doi:10.1016/j.physletb.2006.05.076

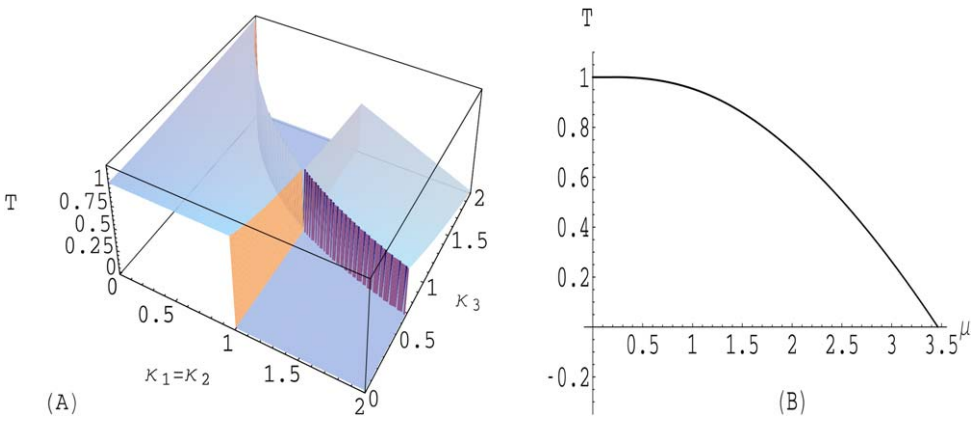

Fig. 1. (A) Critical surface in the space of $((\kappa_1 = \kappa_2 =)\kappa, \kappa_3, T)$. The surface on the hill represents the thermodynamic stable region. (B) Critical line obtained for $(\mu_1 = \mu_2 = \mu_3 =)\mu$ and T. This is the diagonal section of the critical surface in the figure (A). T and μ are scaled by $1/\pi z_m$ and z_m, respectively.

R^3 three space is written as,

$$ds_5^2 = \frac{\mathcal{H}^{-2/3}}{z^2}\left(-f^2(z)\,dt^2 + \mathcal{H}\big(dx^i\big)^2 + \mathcal{H}\frac{dz^2}{f^2(z)}\right), \tag{1}$$

$$f^2(z) = \mathcal{H} - \left(\frac{z}{z_+}\right)^4 \prod_{i=1}^{3}(1+\kappa_i),$$

$$\mathcal{H} = H_1 H_2 H_3, \quad H_i = 1 + \kappa_i\left(\frac{z}{z_+}\right)^2, \quad \kappa_i = q_i z_+^2, \tag{2}$$

where q_i $(i = 1 \sim 3)$ are the charges of three Abelian gauge groups and z_+ represents the smallest value of $f(z) = 0$. The radius of AdS_5 is taken as unit. The Hawking temperature of the background is given by

$$T = \frac{2 + \kappa_1 + \kappa_2 + \kappa_3 - \kappa_1\kappa_2\kappa_3}{2\sqrt{(1+\kappa_1)(1+\kappa_2)(1+\kappa_3)}}T_0, \tag{3}$$

where $T_0 = 1/(\pi z_+)$ denotes the Hawking temperature in the case of the zero chemical potential. Here the chemical potential is defined through the three gauge potentials, $A_t^i(z)$, of the gauged supergravity as

$$\mu_i = A_t^i(z)\big|_{z=z_+} = \frac{\sqrt{2\kappa_i}}{z_+(1+\kappa_i)}\prod_{l=1}^{3}(1+\kappa_l)^{1/2}. \tag{4}$$

Since the bulk configuration depends on the gauge potential, we should consider the thermal properties of the system by considering the Gibbs potential in which the chemical potential is fixed. The density of the Gibbs potential V_G is given as

$$V_G = -\frac{\pi^2 T_0^4}{16 G_5}\prod_{i=1}^{3}(1+\kappa_i). \tag{5}$$

We find from V_G the condition of thermodynamic stability by demanding that the system is on the local minimum point of G in T, μ_i space. This requirement implies the following constraint[1] on κ_i

$$2 - \kappa_1 - \kappa_2 - \kappa_3 + \kappa_1\kappa_2\kappa_3 > 0. \tag{6}$$

[1] We notice that the sign of the last term in Eq. (6) is opposite to the one of [12]. This point is however important.

Although various analyses for this system have been given from the viewpoint of thermodynamics, we consider only the stable region, which satisfies (6), in the parameter space. And we give a critical surface for quark confinement and deconfinement phase transition from a different point of view based on an approximate holographic model.

Our idea is as follows. Usually, the 5d black hole solutions are used to study the high temperature phase of the dual 4d gauge theories without quark confinement. However, for the same black hole solutions, the low temperature phase with confinement can be realized by introducing an infrared cutoff for z, z_m, such as $z_m < z_+$. In this case, the physical region is restricted to the region of $0 < z < z_m$. As a result we can see discrete meson spectra, which are characterized by z_m, and their properties at finite temperature.

On the other hand, for the case of $z_m > z_+$, the physical region is restricted to $0 < z < z_+$ and we find the usual deconfinement background. Then, in this formalism, the critical temperature T_c for the confinement-deconfinement phase transition is given as $T_c = 1/(\pi z_m)$ for the case without the chemical potential. The value of z_m is determined by using some experimental data of meson mass, for example by the vector meson (ρ meson) mass, and we obtain $T_c \sim 100$ MeV.

When the chemical potentials are introduced by the model given above, we obtain in a similar way the critical surface as

$$T_c = \frac{2 + \kappa_1 + \kappa_2 + \kappa_3 - \kappa_1\kappa_2\kappa_3}{2\sqrt{(1+\kappa_1)(1+\kappa_2)(1+\kappa_3)}}\frac{1}{\pi z_m}. \tag{7}$$

This is considered in the 4d parameter space of temperature and three chemical potentials. In order to visualize it, we give a typical example of such a critical surface in a 3d parameter space for $\kappa_1 = \kappa_2$ in Fig. 1.

The surface on the hill in Fig. 1(A) represents the critical surface on which the black hole solution is thermodynamically stable. Outside of this hill, the bottom region of the valley, the R-charged black hole is considered to be unstable. So we must consider some other background in this region. We fortunately find an interesting slice given by the section of $\kappa_1 = \kappa_2 = \kappa_3 = \kappa$, from $(T, \kappa) = (1, 0)$ to $(0, 2)$, on the critical surface. This section provides a phase diagram similar to the one expected in QCD. It is shown in Fig. 1(B).

Hereafter, we make analyses on the special section, and the κ (μ) and the T dependence of various physical quantities are studied.

3. Meson spectra

We consider the 5d meson-action proposed in [4,5] but use the background (1) to treat the system of finite T and κ. The meson action is

$$S_{\rm meson} = \int d^4x\, dz\, \sqrt{-g}\,{\rm Tr}\Big[-\frac{1}{4g_5^2}\big(L_{MN}L^{MN}+R_{MN}R^{MN}\big) - |D_M\Phi|^2 - M_\Phi^2|\Phi|^2\Big], \tag{8}$$

where the case of two flavors ($N_f = 2$) is considered; notations are the same as in [9]. This action is considered as the quark part represented by the probe brane in the string theory. And the fields on the brane is considered to represent meson states composed of a quark–antiquark pair.

3.1. Scalar field

The scalar is defined as $\Phi = Se^{i\pi^a\tau^a}$ and $v(z) \equiv 2\langle S\rangle$. The 5d mass of Φ is $M_\Phi^2 = -3$, since the bulk field corresponds, in the gauge theory side, to an operator with the conformal dimension $\Delta = 3$. The equation of motion for v is obtained as

$$\left[\partial_z^2 + \frac{z^3}{f^2}\partial_z\left(\frac{f^2}{z^3}\right)\cdot\partial_z + \frac{3\mathcal{H}^{1/3}}{z^2 f^2}\right]v(z) = 0, \tag{9}$$

and v is numerically evaluated in this Letter. The asymptotic form near $z = 0$ is $v(z) \sim m_q z + cz^3$, since the background (1) tends to the AdS background there. Two constants, m_q and c, are identified with the quark mass and the chiral condensate, respectively.

The v diverges logarithmically at $z = z_+$ because of the factor f. We have confirmed it explicitly for the case of $T > 0$ and $\kappa = 0$ [9] with the analytic solution of $v(z)$, and numerically for the case of finite κ. However, we can evade the dangerous region $z \sim z_+$, when z_+ is larger than z_m to some extent. The present analysis is then focused on the case $z_+ \gtrsim 1.1 z_m$ for which the logarithmic divergence is not realized in the physical region $z_0 < z < z_m$. In analyses shown below, we fix T and see the κ dependence of physical quantities, since the T dependence has already been discussed in the case of $\kappa = 0$ [9]. So the case $z_+ \gtrsim 1.1 z_m$ is realized in the lower κ region, say $\kappa \lesssim 0.9\kappa_c(T)$, where the critical density $\kappa_c(T)$ is a function of T and satisfies the condition $z_+ = z_m$ for each T, that is

$$z_m = \frac{2 + 3\kappa_c(T) - \kappa_c(T)^3}{2(1+\kappa_c(T))^{3/2}}\frac{1}{\pi T}. \tag{10}$$

The treatment of the dangerous region near $\kappa = \kappa_c(T)$ will be discussed later.

In the present framework, without any inconsistency, we can allow parameters m_q and c to depend on T and κ. However, we do not find a way of determining the T and the κ dependence, although in real QCD we know that the chiral condensate c does depend on T. This point is the defect of the present model. In the present analysis, we simply assume m_q and c are constant in the region $\kappa \lesssim 0.9\kappa_c(T)$. This would be a reasonable assumption for m_q, but it is just a simplification for c.

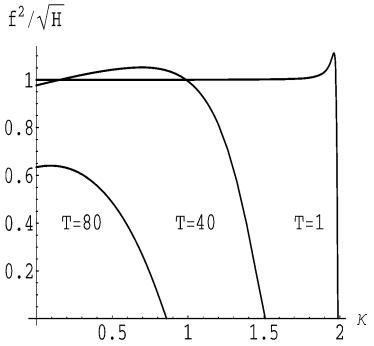

Fig. 2. The κ dependence of $f^2/\sqrt{\mathcal{H}}$ with T fixed. Three curves correspond to three cases of $T = 1$, 40, 80 MeV, respectively. Note that $\kappa_c = 1.989$ for the case of $T = 1$ MeV, 1.509 for $T = 40$ MeV and 0.858 for $T = 80$ MeV.

The fluctuation of S, which is defined as $S = v(z)/2 + \sigma$, can be observed as a singlet meson state (σ). Here and hereafter we consider the static mode, $\partial_i\phi = 0$, for any field ϕ in order to derive the mass in a simple way. So the invariant mass, or pole mass, is defined here as $-\partial_t^2\phi = m^2\phi$. Then the equation for σ is given by adding this 4d mass term to Eq. (9) as

$$\left[\partial_z^2 + \frac{z^3}{f^2}\partial_z\left(\frac{f^2}{z^3}\right)\cdot\partial_z + \frac{3\mathcal{H}^{1/3}}{z^2 f^2} + \frac{\mathcal{H}}{f^4}m^2\right]\sigma = 0. \tag{11}$$

This equation is independent of $v(z)$. The improvement of this defect is postponed to the future.

The discrete mass-spectrum is obtained by solving this equation with the boundary conditions, $\sigma(z)|_{z_0} = \partial_z\sigma(z)|_{z_m} = 0$, where z_0 is the UV cutoff which is taken to zero after all. The mass depends on z_m, T and κ. First, we determine the value of z_m so as to reproduce ρ meson mass at $T = \kappa = 0$. The resultant value is $1/z_m = 0.323$ GeV [7]. It is then possible to estimate the κ dependence of σ meson mass.

The κ dependence of m is predictable from Eq. (11). In the equation, the mass term $m^2\mathcal{H}/f^4$ will have a strong κ dependence through the factor f^4, if m has no κ dependence. However, the mass term should have a weaker κ dependence, since so do the other terms. Hence, the strong κ dependence of f^4 is suppressed by that of m in the mass term, indicating that the κ dependence of m becomes similar to that of $f^2/\sqrt{\mathcal{H}}$.

Fig. 2 shows the κ dependence of the factor $f^2/\sqrt{\mathcal{H}}$ with T fixed. Three curves correspond to three cases of $T = 1$, 40, 80 MeV, respectively. The κ varies in a region $0 \leqslant \kappa < \kappa_c$. The phase transition takes place when $\kappa = \kappa_c$. For lower T cases such as $T = 40$ and 1 MeV, as κ increases, the factor increases once and finally tends to zero in the limit of $\kappa = \kappa_c$.

The κ dependence of $f^2/\sqrt{\mathcal{H}}$ is compared with that of m calculated numerically. The latter is shown in Fig. 3 for the case of $T = 40$ MeV. The κ dependences of m is found to be similar to that of $f^2/\sqrt{\mathcal{H}}$. This similarity is true for other T. Thus, we can see a tendency that m decreases as κ goes to κ_c.

For σ meson, it is possible to take the Dirichlet condition $\sigma(z)|_{z_m} = 0$. It makes m larger by $\sim 50\%$, but the

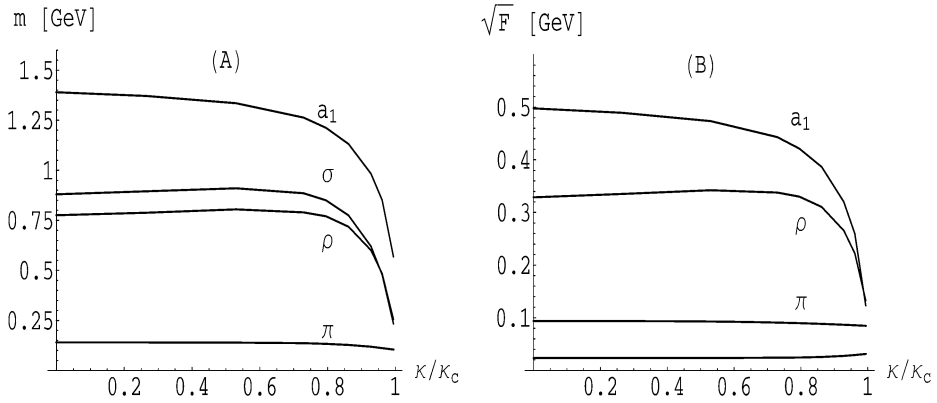

Fig. 3. The κ dependence of masses and decay constants with $T = 40$ MeV fixed. In (A) the curves show m_π, m_ρ, m_σ and m_{a_1} from the bottom. In (B), the curves denote $F_\pi^t/2$, F_π^s, $\sqrt{F_\rho}$ and $\sqrt{F_{a_1}}$ from the bottom. The F_π^t increases as κ goes to κ_c, while F_π^s decreases. Other parameters are fixed as $m_q = 2.26$ MeV and $c = (0.333\ \text{GeV})^3$.

κ-dependence of m is similar to the case of the Neumann condition.

3.2. Vector meson

The gauge bosons are separated to the vector and the axial vector, V_M and A_M, and are defined as $L_M \equiv V_M + A_M$ and $R_M \equiv V_M - A_M$, respectively.

First of all, we consider the vector mesons. The linearized equation for the spatial component V_i is given as

$$\left[\frac{m^2\mathcal{H}}{f^4} + \partial_z^2 + \frac{z\mathcal{H}^{1/3}}{f^2}\partial_z\left(\frac{f^2}{z\mathcal{H}^{1/3}}\right)\cdot\partial_z\right]V_i = 0, \tag{12}$$

where $V_z = 0$ gauge is taken. We adopt the same boundary condition $V_i(z)|_{z_0} = \partial_z V_i(z)|_{z_m} = 0$ as the case of the scalar meson. This equation yields the discrete eigenvalues $m^2 = m_n^2$ under the boundary condition. In order to see the decay constants, it is convenient to expand $V_i(x,z)$ as $V_i(x,z) = \sum_n V_i^{(n)}(x)h_n^V(z)$ for each mass eigenstate. The spatial component of the wavefunction for each mode is normalized as

$$\int_{z_0}^{z_m} dz \frac{\mathcal{H}^{2/3}}{zf^2}\left(h_n^V(z)\right)^2 = 1. \tag{13}$$

The factor $\mathcal{H}^{2/3}/(zf^2(z))$ in the integrand is important in the sense that it determines the κ dependence of the decay constant F_ρ.

Eq. (12) is also independent of $v(z)$, and the κ-dependence of the lowest mass, which is identified with ρ meson mass, is shown in Fig. 3. The ρ-meson mass vanishes or becomes small as κ goes to κ_c because of the mass term $m^2\mathcal{H}/f^4$.

3.3. Axial-vector meson and π-meson

The linearized equations of motion for the axial vector A_μ and the pion π are obtained as

$$\left[\frac{m_a^2\mathcal{H}}{f^4} + \partial_z^2 + \frac{z\mathcal{H}^{1/3}}{f^2}\partial_z\left(\frac{f^2}{z\mathcal{H}^{1/3}}\right)\cdot\partial_z - g_5^2\frac{\mathcal{H}^{1/3}v^2}{z^2f^2}\right]A_{i\perp} = 0, \tag{14}$$

$$\left[\partial_z^2 + \frac{z}{\mathcal{H}^{2/3}}\partial_z\left(\frac{\mathcal{H}^{2/3}}{z}\right)\cdot\partial_z - g_5^2\frac{\mathcal{H}^{1/3}v^2}{z^2f^2}\right]A_{0\perp} = 0, \tag{15}$$

$$\left[\partial_z^2 + \frac{z}{\mathcal{H}^{2/3}}\partial_z\left(\frac{\mathcal{H}^{2/3}}{z}\right)\cdot\partial_z\right]\varphi - g_5^2\frac{\mathcal{H}^{1/3}v^2}{z^2f^2}(\pi+\varphi) = 0, \tag{16}$$

$$m_\pi^2\partial_z\varphi + g_5^2\frac{v^2f^2}{\mathcal{H}^{2/3}z^2}\partial_z\pi = 0, \tag{17}$$

where A_μ is decomposed into the transverse and the longitudinal part, $A_\mu = A_{\mu\perp} + \partial_\mu\varphi$, and $A_z = 0$ gauge is taken. For simplicity, flavor index is neglected and g_5 is determined from the vector current two-point function at $T = \kappa = 0$ [4]. These equations are solved numerically under the boundary conditions, $A_{\mu\perp}(z_0) = \partial_z A_{\mu\perp}(z_m) = 0$ and $\varphi(z_0) = \partial_z\varphi(z_m) = \pi(z_0) = 0$.

Differently from the case of vector and σ mesons, the quantities of axial-vector and pion depend on five parameters m_q, c, z_m, T and κ through $v(z)$, $f(z)$ and $\mathcal{H}$ as seen in Eqs. (14)–(17). For the consistency between the vector and axial-vector meson sectors, here we take the same z_m as in the vector meson sector. Parameters, m_q and c, are determined to reproduce the experimental values, $\bar{m}_\pi$ and $\bar{F}_\pi$, of m_π and F_π at $T = \kappa = 0$; the resultant values are $m_q = 2.26$ MeV and $c = (0.333\ \text{GeV})^3$. This parameter set reproduces masses and decay constants of π, σ, ρ, a_1 mesons at $T = \kappa = 0$ within $\sim 10\%$ error [3,4]. The present model is also successful in reproducing the T dependences of masses and decay constants of π and ρ mesons calculated with the model-independent methods such as lattice QCD calculation [20] and the chiral perturbation theory [19].

In principle, the chiral condensate c depends on T and κ, but we simply assume that c is independent of T and κ. As shown in Fig. 3, masses of axial-vector meson (a_1) and pion also become small as κ goes to κ_c.

3.4. Decay constants

The decay constants are obtained from the wave functions as [4,9]

$$F_{a_n}^2 = \frac{1}{g_5^2}\left[\frac{d^2h_n^A}{dz^2}\bigg|_{z_0}\right]^2, \qquad \left(F_\pi^{t,s}\right)^2 = -\frac{1}{g_5^2}\frac{\partial_z A_{0,i\perp}^{(0)}}{z}\bigg|_{z_0},$$

where $A_{i\perp}(x,z)=\sum_{n\geqslant 1}\alpha_i^{(n)}(x)h_n^A(z)$ and $h_n^A(z)$ is normalized as $h_n^V(z)$ given in (13). Furthermore, $A_{0\perp}^{(0)}$ ($A_{i\perp}^{(0)}$) is the solution to Eq. (15) (Eq. (14) with $m_a^2=0$), satisfying $A_{0,i\perp}^{(0)}(z_0)=1$ and $\partial_z A_{0,i\perp}^{(0)}(z_m)=0$, and $F_\pi^{t,s}$ are the timelike and spatial components of the pion decay constant. Obviously, F_π^t and F_π^s are different from each other at finite T or κ, while $F_\pi^t=F_\pi^s$ at $T=\kappa=0$.

We can see from Fig. 3 that the pion decay constants decreases as κ increases. Eventually, we find $m(\kappa)/m(0)\sim F(\kappa)/F(0)$. Note that F_π^t goes up slowly as κ increases. This is an exception and important in determining the κ dependence of pion velocity v_π, as mentioned later.

3.5. GOR relation and pion velocity

In real QCD, a generalized GOR relation, $m_\pi^2F_\pi^{t2}=2m_qc$, is expected for finite T [19,21]. In the previous work [9], we confirmed that the relation is realized in our model for the case of $T>0$ and $\kappa=0$. It is then of interest whether the relation persists even for finite κ. This is tested by calculating m_π and F_π^t numerically. Fig. 4 shows the m_q dependence of m_π^2 and $2m_qc/F_\pi^{t2}$ by the solid line and the closed circles, respectively. Here the case of $T=40$ MeV and $\kappa=0.8\kappa_c$ is taken as an example. The $m_\pi^2(T)$ shown by the solid line tends to zero as m_q decreases, as a reflection of the Nambu–Goldstone theorem at finite T and κ. Comparing the solid line and the closed circles, one can see that the generalized GOR relation is satisfied.

The pion velocity v_π in the thermal medium with finite μ can be estimated analytically in the chiral limit, $m_q=0$, from F_π^t and F_π^s as $v_\pi=F_\pi^s/F_\pi^t$ [21,22]. In the outer region of the critical line, i.e. when $\kappa>\kappa_c$, we expect the restoration of chiral symmetry. So we can set as $v(z)=0$ for any κ near κ_c, at least when the transition is the second order. This v has no divergence, even when $z_+=z_m$. We can then consider the limit $\kappa\to\kappa_c(T)$. The solutions of Eqs. (14) and (15) are given, under the boundary conditions $A_{i,0}|_{z=0}=1$, as

$$A_i=1+b_i\int_0^z dz_1\frac{z_1\mathcal{H}^{1/3}}{f^2},\tag{18}$$

$$A_0=1+b_0\int_0^z dz_1\frac{z_1}{\mathcal{H}^{2/3}}.\tag{19}$$

The constants $b_{0,i}$ are determined by the boundary conditions, $\partial_z A_{i,0}|_{z=z_m}=\epsilon$, and the limit $\epsilon\to 0$ is taken after obtaining v_π. We then get

$$v_\pi^2=\frac{f^2(z_m)}{\mathcal{H}(z_m)}=1-\left(\frac{z_m}{z_+}\right)^4.\tag{20}$$

We are now considering the limit of $z_+\to z_m$, so v_π^2 approaches to zero linearly with respect to the difference z_+-z_m. This implies ${v_\pi}^2\propto 1-\frac{T}{T_c}$ for the path of $z_+\to z_m$ with κ fixed and that ${v_\pi}^2\propto\kappa_c-\kappa$ for the path with T fixed. Then we can assure the critical exponent $\nu=1$ for both cases.

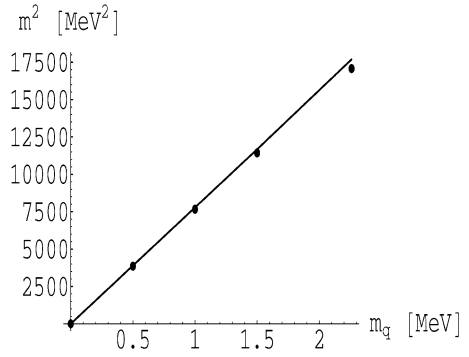

Fig. 4. The m_q dependence of m_π^2. Other parameters are fixed at $T=40$ MeV, $\kappa=0.8\kappa_c$, $\kappa_c=1.509$ and $c=(0.333\ \text{GeV})^3$. The solid line corresponds to $m_\pi^2(\kappa)$ and the closed circles to $2m_qc/F_\pi^{t2}(\kappa)$.

Finally, in the chiral limit, we discuss the behavior of the chiral condensate c near $\kappa=\kappa_c(T)$. When c is finite, $v(z)$ diverges at $z=z_+$, although the divergence is logarithmic and then very weak. When $\kappa=\kappa_c(T)$, the divergence is realized in the present model which considers the region $z_0<z<z_m$. As mentioned above, the κ dependence of c is not determined within the present model. However, if the deconfinement transition and the chiral one take place simultaneously at $\kappa=\kappa_c(T)$ and the chiral transition is the second order, we might evade the logarithmic divergence of $v(z)$, since c is considered to tend to zero more strongly as κ approaches $\kappa_c(T)$. In this situation, we can evaluate v_π at $\kappa=\kappa_c(T)$.

4. Summary

In this Letter, we constructed a holographic model of gauge theory at finite temperature with nonzero chemical potential (μ) conjugate to R-charge density (κ), introducing the five-dimensional R-charged black hole solution of Behrndt, Cvetič and Sabra. The gauge theory thus constructed has two phases, confinement and deconfinement ones. The phase diagram of the gauge theory is richer than that of QCD in the sense that the gauge theory has three chemical potentials conjugate to R-charge densities while QCD has only one chemical potential conjugate to the baryon number density. In the three-dimensional phase diagram of the gauge theory, a special section is similar to the one expected in QCD.

The present model makes it possible to evaluate meson masses and decay constants nonperturbatively even in the thermal system with nonzero chemical potential. We then calculated these quantities in the confinement phase of the special section and found that these quantities decrease as R-charge density κ increases with T fixed. Furthermore, we confirmed that the Nambu–Goldstone theorem and the generalized Gell-Mann–Oakes–Renner relation persist in the thermal system with finite chemical potential.

We estimated the pion velocity as $v_\pi=0$ on the critical line of the phase diagram, assuming that the deconfinement phase transition and the second-order chiral one take place simultaneously. The present result is consistent with the result of Son and Stephanov [22] based on the sigma model, but somewhat

deviates from the result of Ref. [23]. However, the present result supports the statement that the measured pion velocity 0.65 [24], deduced from the pion spectra observed by STAR [18] at RHIC, would be a signal of QCD phase transition.

The present model has two defects. One is that the profile function $v(z)$ diverges on the critical line, although the divergence is logarithmic and then very weak. The other is that the T and the κ dependence of c are not determined within the present model. As for the chiral limit, however, if the deconfinement phase transition and the second-order chiral one take place simultaneously, we can expect that c tends to zero as T and κ approach the critical line. For such a vanishing c, we can expect that $v(z)$ does not diverge on the critical line and then that the present model becomes reliable even near the line. So it is quite interesting to find a way of determining the T and the κ dependence of c in the present holographic model or its extension.

Finally we comment on the bold procedure, the hard IR cutoff, which is essential in the present model. This cutoff seems to be bold, but we could understand it very naturally. The action $S_{\rm meson}$, Eq. (8), is regarded as the effective 5d action for the probe brane(s). In the phase of chiral symmetry breaking, we find a minimum value of r, r_m, for the probe brane by solving its profile function [2], so the theory on the brane should be restricted to the region $r_m < r$. This r_m could be identified with the IR cutoff introduced in the present model.

Acknowledgements

This work has been supported in part by the Grants-in-Aid for Scientific Research (13135223) of the Ministry of Education, Science, Sports, and Culture of Japan.

References

[1] J.M. Maldacena, Adv. Theor. Math. Phys. 2 (1998) 231, Int. J. Theor. Phys. 38 (1999) 1113, hep-th/9711200;
S.S. Gubser, I.R. Klebanov, A.M. Polyakov, Phys. Lett. B 428 (1998) 105, hep-th/9802109;
E. Witten, Adv. Theor. Math. Phys. 2 (1998) 253, hep-th/9802150.
[2] A. Karch, E. Katz, JHEP 0206 (2002) 043;
M. Kruczenski, D. Mateos, R.C. Myers, D.J. Winters, JHEP 0307 (2003) 049;
M. Kruczenski, D. Mateos, R.C. Myers, D.J. Winters, JHEP 0405 (2004) 041;
J. Babington, J. Erdmenger, N.J. Evans, Z. Guralnik, I. Kirsch, Phys. Rev. D 69 (2004) 066007;
N.J. Evans, J.P. Shock, Phys. Rev. D 70 (2004) 046002;
C. Nunez, A. Paredes, A.V. Ramallo, JHEP 0312 (2003) 024;
T. Sakai, S. Sugimoto, Prog. Theor. Phys. 113 (2005) 843;
K. Ghoroku, M. Yahiro, Phys. Lett. B 604 (2004) 235.
[3] K. Ghoroku, T. Sakaguchi, N. Uekusa, M. Yahiro, Phys. Rev. D 71 (2005) 106002.
[4] J. Erlich, E. Katz, D.T. Son, M.A. Stephanov, hep-ph/0501128.
[5] L. Da Rold, A. Pomarol, Nucl. Phys. B 721 (2005) 79, hep-ph/0510268.
[6] G.F. de Teramond, S.J. Brodsky, Phys. Rev. Lett. 94 (2005) 201601.
[7] K. Ghoroku, N. Maru, M. Tachibana, M. Yahiro, hep-ph/0510334.
[8] E. Katz, A. Lewandowski, M.D. Schwartz, hep-ph/0510388.
[9] K. Ghoroku, M. Yahiro, hep-ph/0512289.
[10] K. Behrndt, M. Cvetič, W.A. Sabra, Nucl. Phys. B 553 (1999) 317, hep-th/9810227.
[11] R.V. Gavai, S. Gupta, Phys. Rev. D 68 (2003) 034506, hep-lat/0303013.
[12] D.T. Son, A.O. Starinets, hep-th/0601157.
[13] P. Kovtun, D.T. Son, A.O. Starinets, JHEP 0310 (2003) 064, hep-th/0309213.
[14] S.S. Gubser, Nucl. Phys. B 551 (1999) 667, hep-th/9810225.
[15] A. Chamblin, R. Emparan, C.V. Johnson, R.C. Myers, Phys. Rev. D 60 (1999) 064018, hep-th/9902170.
[16] M. Cvetič, S.S. Gubser, JHEP 9904 (1999) 024, hep-th/9902195.
[17] R.G. Cai, K.S. Soh, Mod. Phys. Lett. A 14 (1999) 1895, hep-th/9812121.
[18] J. Adams, et al., STAR Collaboration, Phys. Rev. Lett. 92 (2004) 112301.
[19] D. Toublan, Phys. Rev. D 56 (1997) 5629.
[20] F. Karsch, Nucl. Phys. B (Proc. Suppl.) 83 (2000) 14.
[21] R.D. Pisarski, M. Tytgat, Phys. Rev. D 54 (1996) 2989.
[22] D.T. Son, M.A. Stephanov, Phys. Rev. Lett. 88 (2002) 202302.
[23] M. Harada, M. Rho, C. Sasaki, hep-ph/0506092.
[24] J.G. Cramer, G.A. Miller, J.M.S. Wu, J.H.S. Yoon, Phys. Rev. Lett. 94 (2005) 102302.